PAPER

A hybrid Body-Machine Interface integrating signals from muscles and motions

IOP Publishing J. Neural Eng. 17 (2020) 046004 https://doi.org/10.1088/1741-2552/ab9b6c

Journal of Neural Engineering

OPEN ACCESS

RECEIVED
10 March 2020

REVISED
18 May 2020

ACCEPTED FOR PUBLICATION
10 June 2020

PUBLISHED
8 July 2020

PAPER

A hybrid Body-Machine Interface integrating signals from muscles and motions

Fabio Rizzoglio[1,2,3,6], **Camilla Pierella**[1,4], **Dalia De Santis**[2,3,5], **Ferdinando Mussa-Ivaldi**[2,3] and **Maura Casadio**[1]

[1] Department of Informatics, Bioengineering, Robotics and Systems Engineering, University of Genoa, 16145, Genoa, Italy
[2] Department of Physiology, Feinberg School of Medicine, Northwestern University, Chicago, IL 60611, United States of America
[3] Shirley Ryan Ability Lab, Chicago, IL 60611, United States of America
[4] Bertarelli Foundation Chair in Translational Neuroengineering, Center for Neuroprosthetics and Institute of Bioengineering, School of Engineering, Ecole Polytechnique Federale de Lausanne (EPFL), Geneva 1202, Switzerland
[5] Department of Robotics, Brain and Cognitive Sciences, Istituto Italiano di Tecnologia, Via Enrico Melen 83, 16152, Genoa, Italy
[6] Author to whom any correspondence should be addressed.

E-mail: fabio.rizzoglio@edu.unige.it

Keywords: human-machine interface, motor control, electromyography, motor learning, body-machine interface

Supplementary material for this article is available online

Abstract

Objective. Body-Machine Interfaces (BoMIs) establish a way to operate a variety of devices, allowing their users to extend the limits of their motor abilities by exploiting the redundancy of muscles and motions that remain available after spinal cord injury or stroke. Here, we considered the integration of two types of signals, motion signals derived from inertial measurement units (IMUs) and muscle activities recorded with electromyography (EMG), both contributing to the operation of the BoMI. *Approach.* A direct combination of IMU and EMG signals might result in inefficient control due to the differences in their nature. Accordingly, we used a nonlinear-regression-based approach to predict IMU from EMG signals, after which the predicted and actual IMU signals were combined into a hybrid control signal. The goal of this approach was to provide users with the possibility to switch seamlessly between movement and EMG control, using the BoMI as a tool for promoting the engagement of selected muscles. We tested the interface in three control modalities, EMG-only, IMU-only and hybrid, in a cohort of 15 unimpaired participants. Participants practiced reaching movements by guiding a computer cursor over a set of targets. *Main results.* We found that the proposed hybrid control led to comparable performance to IMU-based control and significantly outperformed the EMG-only control. Results also indicated that hybrid cursor control was predominantly influenced by EMG signals. *Significance.* We concluded that combining EMG with IMU signals could be an efficient way to target muscle activations while overcoming the limitations of an EMG-only control.

1. Introduction

One of the many consequences of spinal cord injury (SCI), stroke and other neurological conditions is the loss of voluntary control of muscles. Impaired voluntary control often manifests with muscle weakness and increase of undesired co-activations of muscles during voluntary contractions [1–3]. The development of such dysfunctional activation patterns affects the ability to perform selective movements and coordinate joint motion, resulting in low performance during functional tasks. Thus, decreasing those abnormal muscle activations, as well as restoring control to neuromuscular regions that have lost cortical input but remain in the zone of partial preservation, become of primary importance. Body-Machine Interfaces (BoMIs) [4, 5] could be valuable instruments to reach this goal, combining assistive and rehabilitative purpose.

BoMIs convert body-derived signals (motion, forces, or neurophysiological activities) into control signals, which in turn are used to operate external devices. As a result, they enable individuals with disabilities to overcome some of their impairments.

The primary use of the BoMI lies in it being an instrument to recover independence after paralysis, although its potential value can also be considered in other situations involving the control of a device by body motions [6] (as in teleoperation [7]). The rationale for the use of body-signals is to maintain and support the engagement of available movements, which is a significant goal after SCI and other neurological conditions. Among the applications of a BoMI, earlier works by our group have focused on the use of motion signals derived from inertial measurement units (IMUs) [8–12]. Although useful for assistive purposes in individuals with impaired functions, IMU signals do not selectively target users' muscle activations. For this purpose, muscles must be explicitly integrated in the control architecture.

Myoelectric interfaces have been widely studied [13], especially in the context of prosthetics [14, 15], but also for rehabilitative purposes [16], both in SCI [17] and stroke [18]. However, EMG signals are inherently noisier than motion signals. The poorer signal-to-noise ratio has an impact on control, leading to a less efficient operation of the external device. To mitigate the effects of neuromuscular noise, one possibility would be to integrate EMG and kinematic signals into a hybrid control system. The combination of IMU and EMG signals has been broadly investigated in the biomedical field. However, most studies have exploited the fusion of EMGs and IMUs for purposes that did not directly involve the use of muscles in the control scheme. IMU and EMG signals have been used together as a mean to improve classifiers for gesture [19] and American Sign Language [20] recognition, as well as capturing the motion of the arm [21]. When muscle activities were used for control, the design of a control map was based on supervised methods, as in the case of a hybrid-based classifier for the control of a computer cursor [22, 23], a trans-humeral prosthesis [24], or a powered wheelchair [25]. This approach, however, limits the user's ability to operate the device in a continuous manner, as the actions to be performed are predefined and not fully tailored to the user's available motor abilities. Unlike supervised algorithms, the BoMI approach proposed the use of an unsupervised control algorithm such as Principal Component Analysis (PCA [26]). In this way, the interface can adapt to one's residual movements and/or muscle activations, potentially facilitating their continuous interaction with the interface.

In the context of BoMIs, the integration of kinematic- and muscle-based control had not been explored yet. In this study, we envisioned a hybrid Body-Machine Interface that would allow to seamlessly switch between kinematic and muscle control modalities. The goal is to provide a way for users to efficiently control the assistive device while maintaining and promoting engagement of selected muscles. In this way, the proposed algorithm would encourage the dual goal of providing the instrument for assistive support and therapeutic intervention.

We developed and tested an interface combining IMU and EMG signals into a hybrid control signal and validated its use for controlling a computer cursor. We tested and compared three different BoMI modalities, IMU-only, EMG-only, and hybrid—IMU and EMG combined, to assess which one would support a more intuitive and easier-to-use interface. Finally, we characterized the motor strategies followed by participants in the three different BoMI modalities and assessed the contribution of the IMU and EMG signals in the hybrid modality.

2. Methods

2.1. Experimental apparatus

This study focused on movements of upper arms and shoulders. Our purpose was to involve more proximal upper limb muscles that are commonly affected by stroke or cervical spinal cord injury and are often targeted by therapeutic interventions [18, 27–31]. In addition, arms and shoulders are easily accessible and offer the opportunity for individuals to operate the interface from a seated position with minimal discomfort. The BoMI recorded eight muscular and eight motion signals bilaterally from the shoulders and upper arms and combined them in two control signals for a computer cursor.

To record motions of the upper body, we used four IMUs (3 Space Sensors, *Yost Labs, Portsmouth, OH, USA*) placed bilaterally on arms and shoulders of each participant as in figure 1. Each IMU sensor was calibrated to transform the raw data from tri-axial accelerometers and gyroscopes into sensor orientation in the Euler-angle format (pitch, roll, and yaw). The calibration was required to optimize the performance of the filters. Since the yaw measurements were affected by drift, we decided to record only the pitch and roll values, which remained stable for the duration of the experiments. To record the muscular activity, we used a 16-channels wireless EMG system (Wave Plus, *Cometa, Milan, Italy*). Muscle activity was digitally acquired via a C# API at a sampling frequency of 2 KHz. We recorded the activity from eight muscles of the left and right arms and shoulders, in particular biceps brachii, lateral triceps, lateral deltoid, and upper trapezius. The raw EMG signals were first bandpass-filtered (2nd order IIR Butterworth, $f_c = 30 - 450$ Hz) to remove high-frequency noise and low-frequency artifacts caused by movement of the electrode relative to the skin. The signals were then rectified and low-pass-filtered (2nd order IIR Butterworth, $f_c = 2$Hz) to obtain the EMGs envelope.

The interface software was developed in C# and based on a multi-threaded architecture to synchronize the acquisition of IMU and EMG signals. The interface consisted of two threads that handled continuous acquisition and online processing of IMU

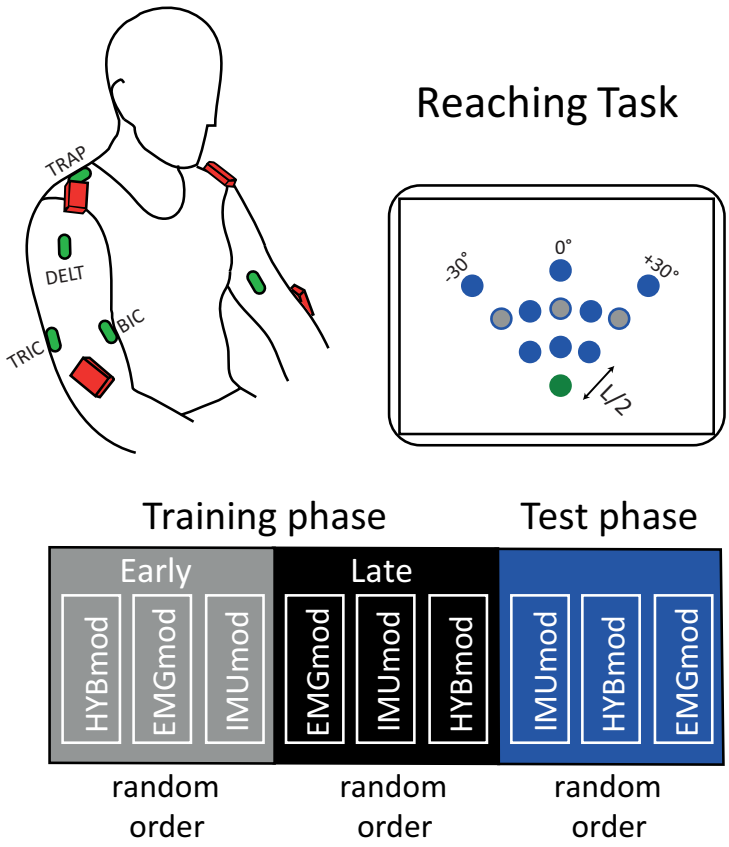

Figure 1. Setup for the reaching task and training protocol. The participant was sitting in front of a computer and was controlling a cursor using signals generated by IMUs (red boxes) and EMG electrodes (green circles). The EMG electrodes are labelled for the right side of the body as follows: biceps-BIC, triceps-TRIC, deltoid-DELT and trapezius-TRAP. Training (grey) and test (blue and grey) targets were presented in a 60° triangular-shape space. Three training targets were set in three different directions (±30°, 0°) at the same distance L of 6 cm from HOME (green) target. Eleven test targets were set in five different directions (±30°, ± 15°, 0°) at three different distances (L/2 = 3, L = 6, and 3L/2 = 9 cm) from HOME target. Thus, during the test phase, participants were asked to reach trained (grey) and untrained (blue) targets.

and EMG signals and a thread to handle cursor control and graphic for a reaching task. The graphical part of the BoMI was developed using OpenTK, a C# graphic library that provided access to graphic tools defined in OpenGL. The update of the graphic frame ran at 50 Hz.

In the BoMI scheme [4], the mapping from body to control signals consisted of two steps: (1) the unsupervised identification of the latent space by dimensionality reduction methods [32–34], (2) the supervised selection of the coordinate system over the latent space based on user's preferences. The dimensionality-reduction method used in this study was PCA.

All participants performed a 60 s guided calibration, during which they were asked to replicate movements of arms and shoulders performed by the experimenter. These movements were performed one at a time (i.e. first shoulder flexion, then shoulder extension, then elbow flexion, etc). This ensured that each participant had a homogenous calibration data set inclusive of all possible joint movements. During the execution of a selected movement, movements of the other joints were not restrained. The instructions were to explore the range of motion without performing extreme or uncomfortable movements. In this phase, both EMG and IMU data were collected and used as a training dataset for the PCA algorithm to derive the control map. Two mappings were computed using kinematic and muscular calibration data independently, in order to control the two-dimensional cursor either with the eight IMU or the eight EMG signals. Each mapping was obtained by applying an eigenvalue decomposition separately of IMU's and EMG's calibration data covariance matrices. The resulting eigenvectors were ordered by the decreasing values of variance accounted for. Thus, the first two eigenvectors—$\boldsymbol{h_1}$ and $\boldsymbol{h_2}$, where $\boldsymbol{h_i}^T = [h_{i,1} \ldots h_{i,8}], i = 1:2$—identified the hyperplanes where the body signals had the greatest variance. The mapping from body-space (IMU or EMG)—$\boldsymbol{q}$, to control-space (x-y coordinates of the cursor)—$\boldsymbol{p}$, followed the same structure as reported in [35, 36]:

$$\boldsymbol{p}_{[2x1]} = \boldsymbol{G}_{[2x2]} \cdot \boldsymbol{H}_{[2x8]} \cdot \boldsymbol{q}_{[8x1]} + \boldsymbol{p0}_{[2x1]}$$

$$\boldsymbol{p} = \begin{bmatrix} \frac{d_1}{\sqrt{\lambda_1}} & 0 \\ 0 & \frac{d_2}{\sqrt{\lambda_2}} \end{bmatrix} \cdot \begin{bmatrix} \boldsymbol{h_1}^T \\ \boldsymbol{h_2}^T \end{bmatrix} \cdot \begin{bmatrix} q_{1,1} \\ \vdots \\ q_{8,1} \end{bmatrix} + \boldsymbol{p_0} \quad (1)$$

To ensure full coverage of the workspace, we included an adjustement $\boldsymbol{G}$ to rescale $\boldsymbol{h_i}$ by the eigenvalues λ_i and the desired width d_1 and height d_2 of the workspace. Moreover, $\boldsymbol{G}$ coud be modified to impose a customized rotation and scaling to the workspace to match participant's preference. The offset vector $\boldsymbol{p_0}$ was chosen to make the origin of the body motion space match a corresponding reference position of the cursor.

We implemented three different BoMI mapping modalities: IMU-only, EMG-only, and hybrid. The following equation defines the cursor position vector, $\boldsymbol{p}$, for all modalities:

$$\boldsymbol{p} = \alpha \boldsymbol{p_{IMU}} + (1-\alpha)\boldsymbol{p_{EMG}} \quad (2)$$

If $\alpha = 1$, the control was carried out by IMUs only (IMUmod), while if $\alpha = 0$, the control was carried out by EMG alone (EMGmod). Values of $0 < \alpha < 1$ implemented a weighted sum of the two modalities of input (HYBmod). Specifically, in our study, the hybrid control was defined with $\alpha = 0.5$ as we aimed to give equal weight to the original and predicted IMU values.

$\boldsymbol{p_{IMU}}$ was the vector containing the coordinates of the cursor obtained by applying PCA to the IMU signals ($\boldsymbol{q_{IMU}}$) as in equation (1). $\boldsymbol{p_{EMG}}$ was defined as a second-degree polynomial of $\boldsymbol{q_{EMG}}$:

$$\boldsymbol{p_{EMG}} = \boldsymbol{W_{EMG}}\boldsymbol{Q_{EMG}} \quad (3)$$

with

$$\boldsymbol{Q_{EMG}} = \begin{bmatrix} 1 \\ \boldsymbol{q_{EMG}} \\ diag\left(\boldsymbol{q_{EMG}}\boldsymbol{q_{EMG}}^T\right) \end{bmatrix} \quad (4)$$

where $\boldsymbol{q_{EMG}}$ is the 8×1 vector of EMG envelopes. $\boldsymbol{W_{EMG}}$ is a 2×17 matrix which elements varied according to the BoMI modality, either EMGmod or HYBmod. In case of EMGmod it was defined as:

$$\boldsymbol{W_{EMG}} = \begin{bmatrix} 0 & \boldsymbol{h}_{1_{EMG}}^T & \boldsymbol{0} \\ 0 & \boldsymbol{h}_{2_{EMG}}^T & \boldsymbol{0} \end{bmatrix} \quad (5)$$

where $\boldsymbol{h}_{i_{EMG}}^T$ were respectively the first and second eigenvectors obtained by applying PCA to $\boldsymbol{q_{EMG}}$. The zero vector $\boldsymbol{0}$ canceled out the quadratic terms $diag\left(\boldsymbol{q_{EMG}}\boldsymbol{q_{EMG}}^T\right)$ in $\mathbf{Q_{EMG}}$. Thus, in EMGmod, equation (3) reduces to equation (1) with $\boldsymbol{p} = \boldsymbol{p_{EMG}}$ representing the vector containing the coordinates of the cursor obtained by applying PCA to EMG ($\boldsymbol{q_{EMG}}$) signals.

For the hybrid modality (HYBmod) we hypothesized that a direct combination of IMU and EMG signals might result in an inefficient control for the user, due to the heterogeneous character of these signals. To encourage a smooth integration and transition between modalities, we decided to transform the EMG signal into an IMU-equivalent signal by using a regression-based approach. In earlier studies, this method has been employed to decode kinematic signals from surface EMG signals used in simultaneous and proportional myoelectric control of prostheses [37, 38]. We implemented a multivariate polynomial regressor, which predicted the cursor coordinates obtained by IMU signals, starting from EMG envelopes. We used a 2nd order polynomial regression to fit the nonlinear relationship between kinematic and muscular signals. Regression was performed on the calibration dataset: the first 30 s were used as training set while the last 30 s were used as test set. We chose to analytically solve the nonlinear regression problem by using the Normal Equation and a L_2 regularization with a least-squares cost function:

$$\boldsymbol{W_{EMG}} = \left(\boldsymbol{Q_{EMG}}^T\boldsymbol{Q_{EMG}} + \lambda \boldsymbol{I}\right)^{-1}\boldsymbol{Q_{EMG}}^T\boldsymbol{p_{IMU}} \quad (6)$$

where $\boldsymbol{Q_{EMG}}$ was defined as in equation (4) and the value of the regularization parameter λ was validated via a search in the range $\left[0 : 10^{-3} : 1\right]$.

2.2. Participants

Fifteen unimpaired participants (eight females, age 23.7 ± 1.39 years) were enrolled in this study. They did not have any known history of neuromotor or musculoskeletal disorders and exhibited typical joint range of motion and muscle strength.

The research was conducted at the University of Genoa in conformity with the ethical standards laid down in the 1964 Declaration of Helsinki for the protection of research subjects and all the study procedures were approved prior the beginning of the study by the local ethical committee (Comitato Etico Regionale—regione Liguria—N. Registro ASL 13/13). According to these procedures, each participant signed a consent form for participating in the study and for the publication of the data in the de-identified form.

2.3. Experimental protocol

The protocol consisted of a reaching task with three different BoMI modalities:

- **IMUmod**—($\alpha = 1$) :the cursor was controlled only by IMU signals;
- **EMGmod**—($\alpha = 0$): the cursor was controlled only by EMG signals
- **HYBmod**—($\alpha = 0.5$): the control of the cursor was shared by IMU and EMG in equal proportion.

IMU and EMG signals were always recorded in every BoMI modality. Participants sit in front of a

15.6″ LCD computer screen, positioned about 1 m away at eye level. The current position of the cursor and targets were displayed on this screen as circles of 0.3 cm and 0.8 cm diameter respectively. Participants were asked to move the cursor over the targets and to remain within each target area for 0.5 s. The reaching task was organized in a center-out, out-center fashion. A new peripheral target was not presented if the cursor was not in the central (HOME) target. This ensured that each center-out motion started from the central target. No time constraint was imposed for reaching the targets. The protocol included two phases of reaching: training and test.

2.3.1. Training phase.
The training phase took place in six reaching epochs—two for each BoMI modality. The order of presentation of each BoMI modality was pseudo-randomized across the six epochs for each participant, such that all three modalities would appear at least once every three epochs. An example of randomization is reported in figure 1. During each epoch, three targets (figure 1, grey targets) positioned at 6 cm from the center of the computer screen were presented in three different directions: 0°, 30°, and −30°. The three peripheral targets were presented twelve times in pseudorandom order, with the condition that each peripheral target was not presented again before all three targets had been reached. Therefore, in this phase participants performed a total of 72 center-out movements for each BoMI modality.

2.3.2. Test phase.
The test phase consisted of three reaching epochs—one for each BoMI modality—with a random order per participant. The goal of this phase was to test if and to what extent participants were able to transfer the skills acquired during the training phase to conditions where they had to move toward (i) different directions and/or (ii) to different displacement amplitudes (scaling-expansion) with respect to the training phase as depicted in blue in figure 1 (blue—untrained and grey—trained targets). Each of the 11 targets was presented four times in pseudorandom order. As shown in figure 1, the targets were distributed radially at three distances from the HOME target (L/2: 3 cm, L: 6 cm and 3L/2: 9 cm) at an angle of ± 30° and 0° (trained directions) and ± 15° (untrained directions, only at distance L). In this phase participants performed a total of 44 center-out movements for each BoMI modality.

2.4. Performance measures
Three different parameters were chosen to evaluate participants' performance:

- **Movement Time (MT):** time to reach the peripheral targets after leaving the HOME target;
- **Linearity Index (LI):** maximum deviation from the straight line connecting the beginning and end of cursor movement divided by nominal distance. This is an index of straightness of cursor movements;
- **Movement Smoothness (MS):** trajectory smoothness was assessed by the number of peaks in the cursor speed profile. We considered every peak larger than a threshold that was set to be 15% of the maximum speed of each trajectory.

2.5. Contribution of IMU and EMG signals in HYB modality
Special focus was given to the hybrid BoMI modality. Since it was defined as the combination of two different signals—IMU and EMG—we studied how these contributed to the participants' performance in HYB-mod. We performed two different types of analysis, one based on cursor position and the other on cursor velocity. We resampled each reaching trial between 0% (when participants exited the HOME target) and 100% (as soon as they entered the peripheral target).

- **Position analysis:** we considered the position of the cursor (p) during reaching and the two contributions to p coming from IMU and EMG signals (p_{IMU} and p_{EMG}) respectively, the latter after applying the regression map. First, we were interested in estimating how IMU and EMG contributed to move the cursor towards the target. We computed the angle between p_{IMU} and p_{EMG} with respect to the peripheral target throughout the entire reaching movement (*angle from target*). Then, we computed the norm of the error between the peripheral target and p_{IMU} and p_{EMG} to assess whether the two contributions decreased monotonically during the whole reaching movement. Finally, we computed the spectrum of the cursor position, p_{IMU} and p_{EMG}, to evaluate the contribution of the IMU and EMG components in the frequency domain.
- **Velocity analysis:** we computed the velocity vectors and their norm (speed) of the cursor v and of its two components v_{IMU} and v_{EMG}. Then we projected v_{IMU} and v_{EMG} onto v. The larger the projection, the stronger the contribution of the corresponding component to the overall velocity of the cursor (expressed as percentage of the overall velocity). We then computed the two angles between v_{IMU} and v and between v_{EMG} and v as an index of *trajectory similarity*.

2.6. Control strategies within each BoMI modality
Beside performance indices, we aimed to evaluate how participants controlled muscles and movements under each of the BoMI modalities. While the reaching task was inherently planar and two-dimensional, participants could reach each target with a theoretically infinite variety of body signal patterns. Here,

by 'control strategy' we intend any particular solution to the reaching task adopted by a participant, that is, any inverse model of the BoMI forward map. Thus, a control strategy transformed a desired position of the cursor (i.e. a target) into a single pattern of body signals driving the cursor in each BoMI modality. We computed the **Variance Accounted For (VAF)**, defined as the percentage of variance of a data set explained by each principal component (PC) during test epochs for each BoMI modality. Considering only two PCs, the higher the value, the more planar the data set. Thus, we used VAF also to evaluate IMU and EMG planarity. We consider planarity to be an important property of these signals: while these are driving the cursor in a planar motion, there is no constraint for them to be planar as well.

Additionally, we investigated how practicing the task with one modality influenced the IMU/EMG signals regardless of their direct participation to cursor control. Specifically, we considered 'control signal' the signal that was actively being mapped into cursor position (e.g. IMU during IMUmod), and 'auxiliary signal' the signal that was recorded but did not contribute to cursor control (e.g. EMG during IMUmod). As our goal was to evaluate how much the control signal changed during training compared to the auxiliary signal, we had to devise a way to compare the variation of two physically incommensurable signals, one referring to the muscle activity, the other to body kinematics. We adopted as measure for this comparison the target information expressed by either IMU or EMG signal, which does not depend on the signal physical dimensions. Thus, we considered the 8D vectors of IMU or EMG signals at the instant when training targets were reached (i.e. **endpoint**). For each of those vectors we trained a classifier (SoftMax regression [39]) to map the body signals, either the control or the auxiliary signals, to their corresponding target. The input of the classifier was a 36×8 matrix, where 36 are the targets reached in both the early and late training of each BoMI modality. Specifically, we trained a classifier on the late training epochs of each BoMI modality (IMUmod, EMGmod, and HYBmod) and tested it on the early training epochs of the same modality (see supplementary materials for more details (available online at stacks.iop.org/JNE/17/046004/mmedia)). Thus, a total of six classifiers were trained, one per each combination of signal and modality. We performed a 6-fold cross validation and computed the **Classification Accuracy (CA)** of each classifier, defined as:

$$CA = \frac{\text{Number of correct classifications}}{\text{Total number of endpoints}}(\%) \quad (7)$$

High values of accuracy were expected if endpoints in early training were similar to those in late training (where the classifiers were trained on). We hypothesized that, since IMU and EMG are physiologically correlated signals, changes in one of them would correspond to changes in the other, regardless of which is the control, and which is the auxiliary signal.

2.7. Statistical analysis

To test the effect of time and BoMI modality on the indicators related to kinematic performance during training, we ran repeated measures ANOVA (rANOVA) with two within-subject factors: BoMI modality (1–3: IMUmod, EMGmod, HYBmod) and time (1–3: early training, late training, test of trained targets L).

To test the effect of the BoMI modality and its interaction with the target position on performance indices during the reaching of untrained targets, we ran a rANOVA with BoMI modality (1–3: IMUmod, EMGmod, HYBmod) and target position (1–3: L/2, 3L/2, other dir L) as within-subject factors. Since movement time and smoothness depended on the target distance, we did not study the effect of the target position for those metrics.

In order to identify the factors that influenced the planarity of the IMU and the EMG signals, we considered the Variance Accounted For by the first two PCs (i.e. planarity) of both signals during the test phase and ran two Friedman tests with body-signal type (1–2: IMU signal, EMG signal) and BoMI modality (1–3: IMUmod, EMGmod, HYBmod) as factors.

To test the differences in the Classification Accuracy between the control and the auxiliary signal, we ran a Wilcoxon signed rank test in each BoMI modality.

We verified that the assumption of running rANOVA were met by testing the sphericity of the data with the Mauchly's sphericity test and the normality of the data with the Anderson-Darling test. All performance metrics data were normally distributed but were not spherical. Thus, we applied Greenhouse-Geisser correction to the p-values. Post-hoc analyses (Fisher's LSD test for rANOVA and Wilcoxon signed ranked test for Friedman) were carried out to verify statistically significant main effects and interactions. The threshold for significance was set at 0.05. All analyses were performed in Statistica (Statsoft, Tulsa, OK, USA).

3. Results

3.1. Performance measures

During training, with practice, all participants reached a higher level of control skill. As shown in figure 2(A), they became faster from first to last training epoch, significantly decreasing the time to reach the targets with each BoMI modality. They also moved the cursor along straighter lines and with increased smoothness in each modality. During the test phase, when reaching targets placed in the trained

Table 1. Table of effects of rANOVA model on each performance index computed on trained targets.

		F	p_{gg}
MT	Modality	2.13	0.154
	Time	24.44	< **0.001**
	Modality: time	0.08	0.942
LI	Modality	1.93	0.178
	Time	18.40	< **0.001**
	BoMI modality: time	0.37	0.746
MS	Modality	5.15	**0.027**
	Time	23.61	< **0.001**
	Modality: time	0.37	0.715

directions, the participants were able to maintain the performance they acquired during late training with each BoMI modality (also figure 2(A)). Results of the rANOVA model are reported in table 1.

Table 2 summarizes the results of rANOVA on test targets. In the test phase, the performance while reaching targets placed in untrained positions was significantly different depending on the BoMI modality. This effect was due to the EMGmod being the hardest modality, while performance during IMUmod and HYBmod resulted comparable for every metric. Moreover, the EMGmod performance in terms of movement time and smoothness degraded significantly more than the other modalities when reaching to further targets (figure 2(B), 3L/2 targets, green bars). The post-hoc analysis is shown in table 2.

3.2. IMU and EMG contribution in HYB BoMI modality

Figure 3(A) depicts the angle between IMU and EMG components of the cursor position with respect to the peripheral target during the hybrid BoMI modalities, while figure 3(C) shows the norm of the error between the actual cursor position and the EMG and IMU components. While the two components started approximately from the same position (close to the HOME target), they steadily diverged with the maximum reached at the end of the reaching movement (figure 3(A)). Interestingly, about halfway through the movement, the norm of the EMG error component became stationary (figure 3(C)), while the norm of the IMU error decreased monotonically throughout the end of the movement. As expected, the frequency analysis proved that the EMG was the noisiest component (figure 3(D)). An example of cursor trajectory for a single reaching movement of one participant is shown in figure 3(B).

Furthermore, the velocity analysis showed that the EMG component of the cursor during the hybrid BoMI modality epochs reached higher speed than the HYB and the IMU component (figure 4(A)). Not only the EMG presented the higher speed, but it also gave the higher contribution during each hybrid BoMI epoch (figure 4(B)). This latter condition was consistent with the EMG trajectory being the closest to the actual hybrid cursor throughout the entire movement (figure 4(C)).

3.3. Control strategies within BoMI modality

Figure 5 summarizes the dimensionality of both IMU and EMG signals during the test phase of each BoMI modality. The variance accounted for by the first two PCs of both signals was consistent across BoMI modalities ($p = 0.627$). However, we found the redundancy of the EMG signal to be inferior to that of the IMU, as a larger amount of variance was explained by its first two components ($p = 0.02$). Post-hoc analysis revealed that this effect was consistent for each modality (IMUmod: $p = 0.018$—figure 5(A), EMGmod: $p = 0.048$—figure 5(B), HYBmod: $p = 0.026$—figure 5(C)). This suggests that EMG signals have a stronger planar (i.e. linear) structure than IMU signals.

Figure 6 summarizes the Classification Accuracy (CA) for the six classifiers trained using EMG and IMU endpoints during the late training phase in each control modality when discriminating among endpoints (or equivalently, among the 3 trained targets) during the corresponding modality in the early training phase. The analysis on body endpoints revealed that the accuracy of a classifier trained on each BoMI modality was the greatest when based on the control signal. Specifically, a classifier trained on IMU endpoints in the late training phase of IMUmod would discriminate targets with significantly higher accuracy than one trained in the same conditions but on EMG endpoints ($p < 0.001$, figure 6(A)). Similarly, a classifier trained on EMG endpoints in the late training phase of EMGmod, would distinguish among targets significantly better than one trained on IMU endpoints ($p < 0.001$, figure 6(B)). Figure 6 shows the accuracy of the two classifiers in HYBmod also. Since in this modality both IMU and EMG signals contributed to cursor control, resulting in no distinction between control and auxiliary signal, we did not run any statistical analysis. It is, however, interesting to note that CA values were in between those obtained during IMUmod and EMGmod. Figure 7 depicts the CA of the classifier trained on IMU endpoints during the late training phase of IMUmod and tested on both IMUmod and HYBmod. Since the regression was transforming EMGs into IMU signals, we wanted to evaluate whether IMU endpoints in IMUmod and HYBmod were comparable. As mentioned earlier, IMU endpoints between early and late training phases of IMUmod were consistent (figures 6(A) and 7, 1st and 2nd column). Interestingly, kinematic endpoints between IMUmod and HYBmod differed, since classification accuracy values dropped (figure 7, 3rd and 4th column).

4. Discussion

This study delivered three main findings: (i) the proposed hybrid control led to comparable performance to IMU-based control and significantly outperformed the EMG-only control; (ii) hybrid cursor

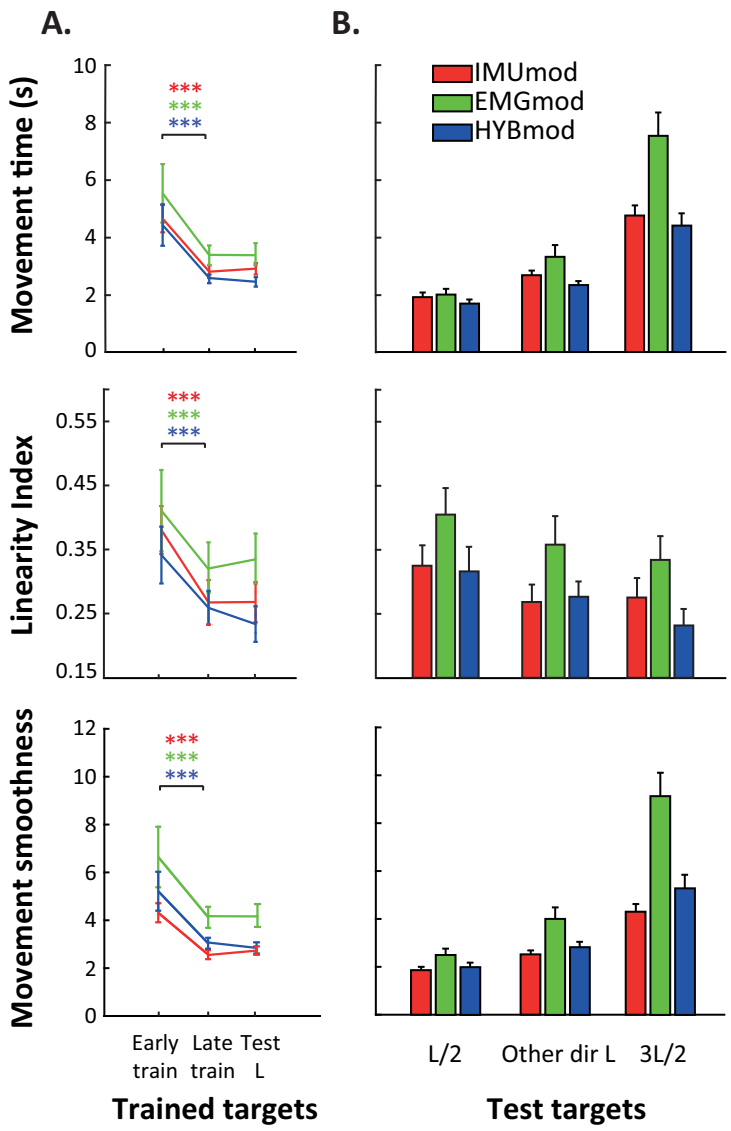

Figure 2. Panel A: Performance measures while reaching targets placed in the trained directions ($\pm 30°$, $0°$) at distance L from HOME during early, late training and test with the three BoMI modalities. Panel B: Performance measures while reaching targets placed in the untrained positions (trained directions at distances L/2 and 3L/2 and untrained directions $\pm 15°$ at distance L) with the three BoMI modalities. Red lines refer to IMUmod, green lines to EMGmod and blue lines to HYBmod. Mean across participants and targets is plotted with standard error. Asterisks represent significant differences as follows: * $0.01 < p < 0.05$, ** $0.001 < p \leqslant 0.01$, *** $p \leqslant 0.001$.

control was predominantly influenced by EMG signals, indicating that combining EMG with IMU signals allows to efficiently target muscle activations, overcoming the limitation of a EMG-based control; (iii) participants were able to effectively identify the physical signals that actually mattered for the cursor control.

4.1. Relevance to rehabilitative therapy

Our novel hybrid control led to the best performance along with the IMU control, confirming our initial hypothesis of motion-preferable control. Thus, our hybrid EMG-IMU control would allow implementing a rehabilitative therapy using joint movements and muscle activities, while at the same time avoiding the performance loss associated with EMG-based control alone. Indeed, in our study, EMG was the least efficient BoMI modality, especially when reaching distal targets. This implies that, while controlling with EMG alone, participants were required to exert and maintain a greater muscle contraction to reach the more distal targets, resulting in a less efficient control. The hybrid modality solved this issue by including the IMU signals in the control scheme, while still maintaining the EMG contribution.

The possibility to directly target muscles for tackling abnormal muscle activations could be achieved by making modifications to the BoMI control map that accounts for EMG contribution (i.e. $\boldsymbol{W_{EMG}}$). Specifically, we could facilitate or discourage the activation of a targeted muscle by assigning a reward/penalty weight to it. The same approach had already been tested with a motion-based BoMI, and it was shown to successfully increase the strength

Table 2. Table of effects of rANOVA model on each performance index computed on test targets.

		F	p_{gg}	Fisher LSD	p
MT	Modality	11.3	**0.003**	IMUmod v EMGmod	**0.001**
				HYBmod v EMGmod	**< 0.001**
				HYBmod v IMUmod	0.357
	Target	132.4	**< 0.001**	L/2 v other dir L, L/2 v 3L/2, 3L/2 v other dir L	**< 0.001**
	Modality * target	7.4	**0.003**	IMUmod (3L/2) v EMGmod (3L/2)	**< 0.001**
				HYBmod (3L/2) v EMGmod (3L/2)	**< 0.001**
				HYBmod (3L/2) v IMUmod (3L/2)	0.420
LI	Modality	4.89	**0.015**	IMUmod v EMGmod	**0.021**
				HYBmod v EMGmod	**0.007**
				HYBmod v IMUmod	0.639
	Target	6.5	**0.005**	L/2 v other dir L	**0.02**
				L/2 v 3L/2	**0.002**
				3L/2 v other dir L	0.299
	Modality * target	0.74	0.572		
MS	Modality	18.7	**< 0.001**	IMUmod v EMGmod	**< 0.001**
				HYBmod v EMGmod	**< 0.001**
				IMUmod v HYBmod	0.265
	Target	99.61	**< 0.001**	L/2 v 3L/2, 3L/2 v other dir L	**< 0.001**
				L/2 v other dir L	**0.006**
	Modality * target	12.69	**< 0.001**	IMUmod (3L/2) v EMGmod (3L/2)	**< 0.001**
				HYBmod (3L/2) v EMGmod (3L/2)	**< 0.001**
				IMUmod (3L/2) v HYBmod (3L/2)	**0.002**

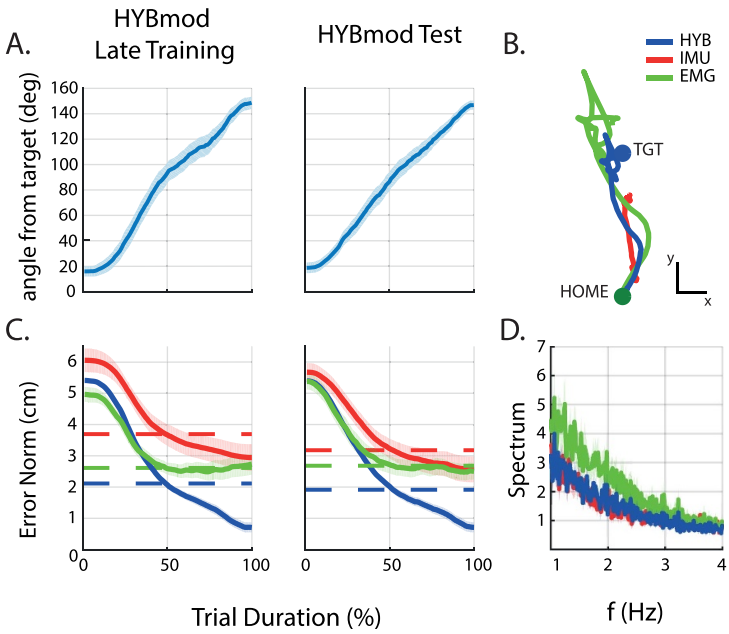

Figure 3. Panel A: Angle between the IMU and EMG components of cursor positions with respect to the peripheral target during hybrid BoMI modalities (late training and test). Panel B: Cursor trajectory of a single reaching movement of one participant during test session of HYBmod. Cursor (blue) is shown together with its IMU (red) and EMG (green) components. Panel C: Norm of the error vector between the peripheral target and the HYB (blue), IMU (red) and EMG (green) components of the cursor position respectively. Dashed lines represent error norm values at 50% of trial duration. Panel D: spectrum of cursor (blue) and its IMU (red) and EMG (green) components during test session of HYBmod. Panels A, C and D show mean values across repetitions, targets and participants against the standard error.

and range of motion of the body side that was more impaired following SCI [40].

Hybrid control was designed to transform EMG envelopes into control signals equivalent to IMU signals so as to obtain smoother transitions between modalities. Interestingly, despite the fact that IMUmod outperformed EMGmod, the EMG signal contributed the most in the hybrid BoMI modality (figure 4(B)). This is additional evidence to validate the rehabilitative potential of the proposed interface, as it demonstrates the prevalent role of muscles in the hybrid control scheme. The EMG input was associated with a higher gain in the hybrid control as it was quickly driving the cursor towards the target (figure 3(C)). On the other hand, the IMU had lower gain but also lower noise (figure 3(D)). Its main effect was

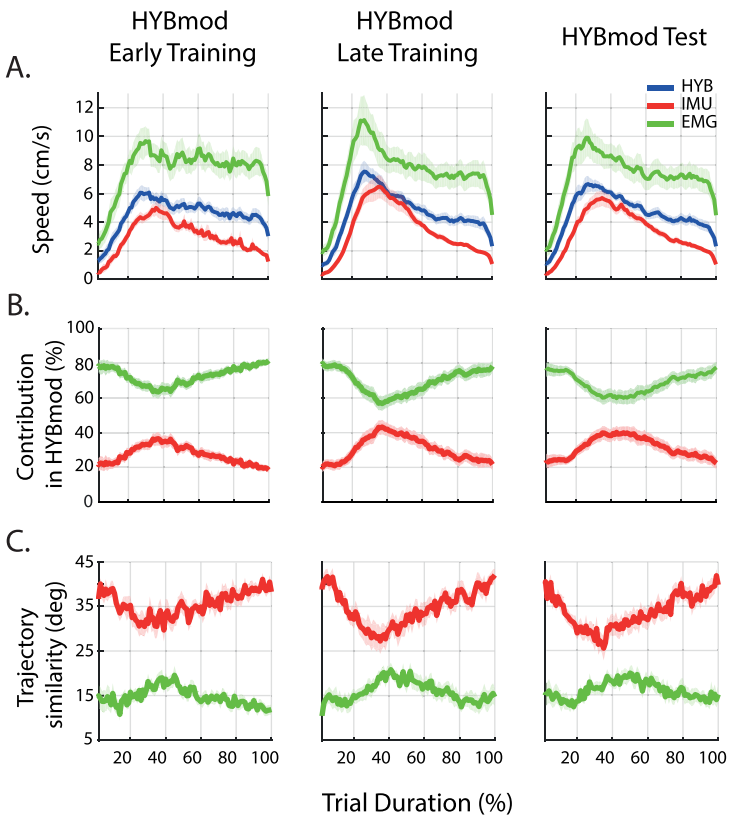

Figure 4. Panel A: Speed of the HYB (blue), IMU (red) and EMG (green) component of the cursor. Panel B: Contribution of IMU (red) and EMG (green) component in the velocity of the cursor. Panel C: Angle values between v and v_{IMU} (red) and between v and v_{EMG} (green). All conditions are shown during hybrid BoMI modalities (early, late training and test). Mean across repetitions, targets and participants is plotted against its standard error.

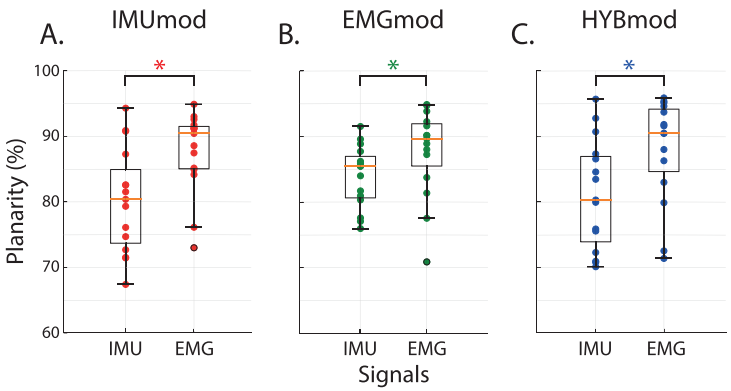

Figure 5. Planarity values for IMU and EMG are shown for each BoMI modality (Panel A: IMUmod, red dots; Panel B: EMGmod, green dots; Panel C: HYBmod, blue dots). Boxplots are showing first quartile, median (yellow), third quartile and outliers. Asterisks represent significant differences as follows: * $0.01 < p < 0.05$, ** $0.001 < p \leqslant 0.01$, *** $p \leqslant 0.001$.

to smoothen the noisier EMG contribution. Thus, hybrid control seems to combine the best of both signals, by exploiting the faster EMG signal in approaching the target and the damping effect of the IMU to reach the target accurately.

We want to note that, while this was a single-day study, use of the interface for assistive as well as rehabilitation purposes will span multiple days. This will inherently pose several challenges, such as the necessity to reposition the IMU and EMG sensors in a similar fashion during consecutive days. Moreover, the main control maps for IMU and EMG-based control, as well as the polynomial regression model needed for the hybrid control, might require day-to-day recalibration. Several techniques have been developed to mitigate the effect of inconsistent electrode placement

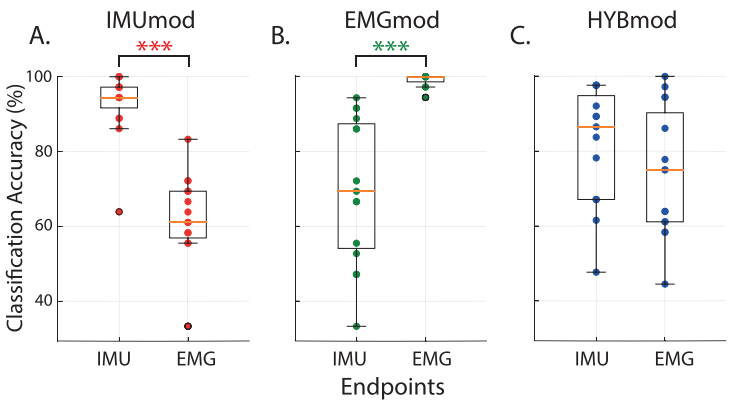

Figure 6. IMUs and EMGs endpoints classification accuracy for IMUmod (Panel A, red dots), EMGmod (Panel B, green dots) and HYBmod (Panel C, blue dots). Each dot represents the CA of an individual participant. Boxplots are showing first quartile, median (yellow), third quartile and outliers. The higher the accuracy in a specific modality, the more similar the endpoints of that body signal between early and late training. Asterisks represent significant differences as follows: * $0.01 < p < 0.05$, ** $0.001 < p \leqslant 0.01$, *** $p \leqslant 0.001$.

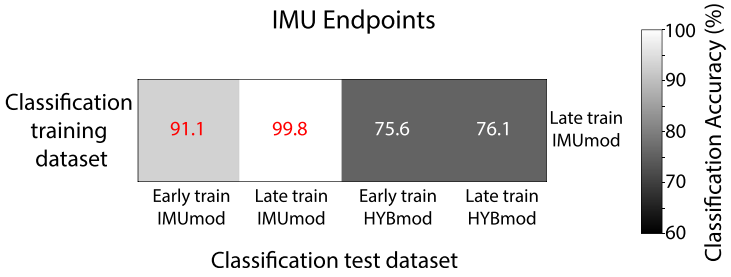

Figure 7. Confusion matrix of classification accuracy for the classifier trained with IMU endpoints on the late training phase of IMUmod. The classifier has been tested on four conditions: during early and late training phases of IMUmod (1st and 2nd column) and during early and late training phases of HYBmod (3rd and 4th column). The higher the accuracy, the more similar the kinematic endpoints between the late training phase of IMUmod and the phase shown in each column.

and recalibration-need in a multi-day sessions scenario [41]. A future iteration of this study should consider integrating those procedures to improve the stability of the interface during the course of a rehabilitation protocol.

4.2. Relevance to basic and transactional neuroscience

While developing new technology to be applied in clinical rehabilitation is a leading motivation for this work, Body-Machine Interfaces have a domain of potential application that includes but is not limited to clinical use. As an example, BoMIs have been used to control a variety of devices, such as drones [6] and robotic arms [7, 42]. Furthermore, there is an important application of this instrument to deepen the understanding of the human motor system. While there is an evident correlation between EMG activity and movement, understanding the causal connection between the two is hampered by complex cascade of neuromuscular, sensory, and biomechanical elements that intervenes between the observed electrical activity and the related limb motions. In this respect, the BoMI offers a unique method to artificially enforce EMG causality on the observed and controlled motion without intervening musculoskeletal dynamics. Our findings suggests (e.g. figure 3) that in this modified causality context, the users gave a leading role to the direct EMG control in the initial part of the movement, while the second phase of the movement, where the cursor was performing the final approach to the target, was driven by the IMU motion signals, which were affected by musculoskeletal dynamics. This can be taken as evidence that the nervous system exploits mechanical properties of the moving body to facilitate the control in the final reaching component. Therefore, the test of the hybrid BoMI in unimpaired participants served the specific purpose of providing a normative baseline for understanding of how these different control signals are organized by the motor control system. This is an essential step to evaluate performance in a population with SCI or other neurological conditions.

4.3. Control strategies within BoMI modality

Numerous studies suggested that our brain, in order to generate actions designed to realize a desired task, develops an internal representation (i.e. the internal model) of the task as the evolution of a dynamical system [43]. A recent study from our group [44]

mathematically described how, in the BoMI context, users not only generate an inverse model of the control map, but that their inverse model converges as a first-order exponential toward a particular state (i.e. a single solution). In this study, we noticed a similar condition. Specifically, participants were required to learn three different inverse models to effectively control the cursor with each of the three different BoMI modalities. When controlling with IMU or EMG signals alone, they succeeded at identifying the physical signals that actually mattered for cursor control, and to distinguish the primary control signal from the auxiliary signal. In other words, the kinematic and muscular endpoints that they held were consistent throughout the training with IMUmod and EMGmod respectively. Thus, in each modality participants converged to an inverse solution of the BoMI mapping EMG or IMU signals onto cursor position. Conversely, the analysis we used could not prove whether participants converged to an inverse solution with HYBmod as well, since in this case there was no distinction between the control and the auxiliary signal. However, it is interesting to note that in HYBmod, with the EMG signals being mapped into the IMU space, participants changed their kinematic endpoints with respect to the IMUmod (figure 7). This is not trivial, as participants could have merely replicated the kinematic endpoints they held in IMUmod. Hence this suggests that muscle activity was greatly contributing to the hybrid control, further supporting the applicability of the interface for rehabilitative purposes.

Our initial hypothesis was that kinematic and muscular endpoints would have consistent behavior due to the physiological correlation between IMUs and EMGs. As such, changes in endpoint in one space should have been reflected in changes in the other, regardless of which was associated with the control signal, and which with the auxiliary signal. However, this discrepancy between the two spaces was indeed present and allowed participants to learn how to operate the interface. As a matter of fact, when participants did not have to rely on the EMG signals as they were operating the interface with the IMU modality, they activated muscles differently while maintaining a similar IMU endpoint at the end of a reaching movement (figure 6(A)). By contrast, when they were involved with the EMG-based control, they showed different IMU endpoints while maintaining consistent muscle activations at the end of a reaching movement (figure 6(B)). We speculate that there is an analogy between results in both conditions and the uncontrolled manifold (UCM) hypothesis [45] and optimal feedback control [46], which state that the controller (i.e. the brain) allows elements to show higher variability as long as this does not affect the desired value of the task, i.e. as long as the elements are auxiliary signals. Specifically, the concept of redundancy plays a key role in explaining our results. On one hand, it is known that a given task can be accomplished with different movement patterns [47] and that a specific movement can be generated by an infinite number of muscle activation combinations [48]. According to the *natural redundancy of muscles* compared to the number of joints, IMU signals are less redundant than EMGs, thus explaining why participants were able to have different EMG activations while maintaining a similar movement strategy. On the other hand, in our task, the EMG signals had a stronger planar structure than the IMUs. This *task-related redundancy* may explain why the participants were able to have different IMU endpoints while maintaining similar muscle activations. The co-existence of these two distinct types of redundancy was merely a result of our experimental setup. In fact, we were recording signals from a subset of muscles of the upper body, thus ignoring others that could have significantly contributed to the overall EMG dimensionality.

4.4. Limitations

We also need to highlight some possible limitations of our hybrid approach. In order to get a smooth transition between IMU and EMG control modalities, a stable regression between those signals is required. Here, we addressed the problem of predicting IMUs from EMGs with a non-linear regression model to accommodate for the natural nonlinear relationship existing between movement and muscle signals. A general approach to handle nonlinear problems is to add more polynomial features (e.g. two in our study) as predictors. Adding polynomial features is simple to implement and can be effective, but the polynomial order to use in the model might be difficult to validate. In this sense, a non-parametric kernel-based regression [49] might be more appropriate to depict this relationship without having to explicitly specify the polynomial order. Furthermore, our approach did not consider the temporal dependency between EMG and IMU. Since EMG is anticipating IMU from a temporal point of view, a model that considers this time-difference might be more robust (e.g. a recurrent neural network [50]). Despite these limitations, we found our particular instance of regression to work properly with unimpaired participants, thus constituting a promising starting point with the potential to be further fine-tuned to increase its robustness.

In previous sections, we discussed how performance with EMG modality resulted in inefficient control especially when reaching the more distal targets, due to the requirement of higher muscle contractions. Note that the control of the cursor was position-based. The exertion of those uncomfortable contractions could have been avoided with a velocity-based control. This could have improved performance during the EMG-only control [51], but it could have, nonetheless, harmed performance when reaching other portions of the workspace. In this sense, more extensive tests should be carried out, possibly

combining our hybrid approach with a velocity-based cursor.

Finally, we want to make one cautionary note regarding our computation of the experimental redundancy. It was defined as the variance accounted for by the first two principal components derived from PCA. While for each BoMI modality the forward map was linear, the control strategy might have been linear or non-linear. While a linear strategy corresponded to a planar manifold embedded within the body signals, a nonlinear strategy corresponded to a curved manifold. Since PCA is a linear algorithm approximating a participant's control strategy with a planar manifold, a nonlinear control strategy would result in signals whose variance cannot be fully accounted for by linear combinations of two principal components. This led to an approximated computation of the experimental redundancy (or planarity, equivalently), and it is a known particular instance of the more general observation that PCA, when applied to a nonlinear dataset, tends to overestimate the dimensionality of the data [52].

5. Conclusion

The proposed interface sets the ground for an unsupervised algorithm that concurrently includes motions and muscles in the control-scheme. Our hybrid approach combines the best features of muscular and kinematic signals, by exploiting the former to quickly move the cursor towards the target and exploiting the damping effect of the latter to reach the target accurately. We also found that muscles were predominantly contributing for the cursor control. This indicates how the interface could be used in rehabilitative protocols to efficiently target muscle activations, without the limitations associated with EMG-based control alone. Moreover, our work showed how participants were able to effectively identify the physical signals that actually mattered for the cursor control, suggesting that they converged to an inverse solution of the BoMI mapping EMG or IMU signals onto cursor position.

Acknowledgments

This work was supported by the Marie Curie Integration Grant (FP7- PEOPLE-2012-CIG-334201), the Ministry of Science and Technology, Israel (Joint Israel-Italy lab in Biorobotics Artificial somatosensorial for humans and humanoids), the National Science Foundation Grant No. 1632259, the NIDILRR Grant 90REGE0005-01, the NICHHD Grant 5R01HD072080 and the European Unions Horizon 2020 research and innovation program under the Marie Sklodowska-Curie, project REBoT, G.A. No. 750464.

The authors of this paper would like to thank Alexandra A Portnova for helpful comments and for proof-reading the manuscript.

ORCID iDs

Fabio Rizzoglio https://orcid.org/0000-0002-6744-4605
Camilla Pierella https://orcid.org/0000-0002-8108-9363

References

[1] Adams M M and Hicks A L Spasticity after spinal cord injury 2005 *Spinal. Cord.* **43** 577–86
[2] Watkins C L, Leathley M J, Gregson J M, Moore A P, Smith T L and Sharma A K Prevalence of spasticity post stroke 2002 *Clin. Rehabil.* **16** 515–22
[3] Cremoux S, Amarantini D, Tallet J, Dal Maso F and Berton E 2016 Increased antagonist muscle activity in cervical SCI patients suggests altered reciprocal inhibition during elbow contractions *Clin. Neurophysiol.* **127** 629–34
[4] Casadio M, Ranganathan R and Mussa-Ivaldi F A 2012 The body-machine interface: A new perspective on an old theme *J. Mot. Behav.* **44** 419–33
[5] Mussa-Ivaldi F A, Casadio M, Danziger Z C, Mosier K M and Scheidt R A 2011 Sensory motor remapping of space in human-machine interfaces *Prog. Brain Res.* **191** 45–64
[6] Miehlbradt J *et al* 2018 Data-driven body–machine interface for the accurate control of drones *Proc. Natl. Acad. Sci. USA* **115** 7913–8
[7] Ajoudani A, Tsagarakis N and Bicchi A 2012 Tele-impedance: teleoperation with impedance regulation using a body-machine interface *Int. J. Rob. Res.* **31** 1642–55
[8] Abdollahi F *et al* 2017 Body-machine interface enables people with cervical spinal cord injury to control devices with available body movements: proof of concept *Neurorehabil. Neural Repair* **31** 487–93
[9] Seáñez-González I *et al* 2016 Body-machine interfaces after spinal cord injury: rehabilitation and brain plasticity *Brain Sci.* **6** 1–19
[10] Pierella C *et al* 2017 Changes in neuromuscular activity during motor training with a body-machine interface after spinal cord injury *IEEE Int. Conf. Rehabil. Robot.* pp 1100–5
[11] Summa S *et al* 2015 A body-machine interface for training selective pelvis movements in stroke survivors: a pilot study *Proc. Annu. Int. Conf. IEEE Eng. Med. Biol. Soc. EMBS* **2015** 4663–6
[12] Thorp E B *et al* 2016 Upper body-based power wheelchair control interface for individuals with tetraplegia *IEEE Trans. Neural Syst. Rehabil. Eng.* **24** 249–60
[13] Vujaklija I, Shalchyan V, Kamavuako E N, Jiang N, Marateb H R and Farina D 2018 Online mapping of EMG signals into kinematics by autoencoding *J. Neuroeng. Rehabil.* **15** 21
[14] Zecca M, Micera S, Carrozza M C and Dario P 2002 Control of multifunctional prosthetic hands by processing the electromyographic signal *Crit. Rev. Biomed. Eng.* **30** 4–6
[15] Fani S *et al* 2016 Assessment of myoelectric controller performance and kinematic behavior of a novel soft synergy-inspired robotic hand for prosthetic applications *Front. Neurorobot.* **10** 1–15
[16] Mulas M, Folgheraiter M and Gini G 2005 An EMG-controlled exoskeleton for hand rehabilitation *Proc. 2005 IEEE 9th Int. Conf. Rehabil. Robot.* **2005** 371–4
[17] Rizzoglio F *et al* 2019 A myoelectric computer interface for reducing abnormal muscle activations after spinal cord injury *IEEE Int. Conf. on Rehabilitation Robotics* pp 1049–54

[18] Wright Z A, Rymer W Z and Slutzky M W 2014 Reducing abnormal muscle coactivation after stroke using a myoelectric-computer interface: a pilot study *Neurorehabil. Neural Repair* **28** 443–51
[19] Georgi M, Amma C and Schultz T 2015 Recognizing hand and finger gestures with IMU based motion and EMG based muscle activity sensing *BIOSIGNALS 2015-8th Int. Conf. Bio-Inspired Syst. Signal Process.* pp 99–108
[20] Wu J, Sun L and Jafari R 2016 A wearable system for recognizing american sign language in real-time using IMU and surface EMG sensors *IEEE J. Biomed. Heal. Informatics* **20** 1281–90
[21] Xu Y, Yang C, Liang P, Zhao L and Li Z 2016 Development of a hybrid motion capture method using MYO armband with application to teleoperation *2016 IEEE Int. Conf. Mechatronics Autom.* pp 1179–84
[22] Forbes T 2013 Mouse HCI Through Combined EMG and IMU *Open Access Master's Theses*, University of Rhode Island, Paper **43**
[23] Xiong A, Chen Y, Zhao X, Han J and Liu G 2011 A novel HCI based on EMG and IMU *2011 IEEE Int. Conf. Robot. Biomimetics,* pp 2653–7
[24] Lauretti C, Davalli A, Sacchetti R, Guglielmelli E and Zollo L 2016 Fusion of M-IMU and EMG signals for the control of trans-humeral prostheses *Proc. IEEE RAS EMBS Int. Conf. Biomed. Robot. Biomechatronics* **2016** 1123–8
[25] Kundu A S, Mazumder O, Lenka P K and Bhaumik S Hand gesture recognition based omnidirectional wheelchair control using IMU and EMG sensors 2018 *J. Intell. Robot. Syst. Theory Appl.* **91** 529–41
[26] Wold S, Esbensen K and Geladi P 1987 Principal component analysis *Chemom. Intell. Lab. Syst.* **2** 37–52
[27] Tropea P, Monaco V, Coscia M, Posteraro F and Micera S 2013 Effects of early and intensive neuro-rehabilitative treatment on muscle synergies in acute post-stroke patients: a pilot study *J. Neuroeng. Rehabil.* **10** 1–15
[28] Hincapie J G and Kirsch R F 2007 EMG-based control for a C5/C6 spinal cord injury upper extremity neuroprosthesis *Annual Int. Conf. of the IEEE Eng. Med. Biol. Proc.* pp 2432–5
[29] Giuffrida J P and Crago P E 2001 Reciprocal EMG control of elbow extension by FES *IEEE Trans. Neural Syst. Rehabil. Eng.* **9** 338–45
[30] Brucker B S and Bulaeva N V 1996 Biofeedback effect on electromyography responses in patients with spinal cord injury *Arch. Phys. Med. Rehabil.* **77** 133–7
[31] Harburn K L and Spaulding S J Muscle activity in the spinal cord-injured during wheelchair ambulation. 1986 *Am. J. Occup. Ther. Off. Publ. Am. Occup. Ther. Assoc.* **40** 629–36
[32] Hyvärinen A and Oja E 2000 Independent component analysis: algorithms and applications *Neural. Networks* **13** 411–30
[33] Kramer M A Nonlinear principal component analysis using autoassociative neural networks 1991 *AIChE J.* **37** 233–43
[34] Schölkopf B, Smola A and Müller K-R 1997 Kernel principal component analysis *Int. Conf. Artificial Neural Netw.* pp 583–8
[35] Farshchiansadegh A *et al* 2014 A body machine interface based on inertial sensors *2014 36th Annu. Int. Conf. IEEE Eng. Med. Biol. Soc.* pp 6120–4
[36] Casadio M *et al* 2010 Functional reorganization of upper-body movement after spinal cord injury *Exp. Brain Res.* **207** 233–47
[37] Krasoulis A, Vijayakumar S and Nazarpour K 2015 Evaluation of regression methods for the continuous decoding of finger movement from surface EMG and accelerometry *Int. IEEE/EMBS Conf. Neural Eng.* **2015** 631–4
[38] Hahne J M *et al* 2014 Linear and nonlinear regression techniques for simultaneous and proportional myoelectric control *IEEE Trans. Neural Syst. Rehabil. Eng.* **22** 269–79
[39] Gao B and Pavel L 2017 On the properties of the softmax function with application in game theory and reinforcement learning (arXiv: 1704.00805)
[40] Pierella C *et al* 2015 Remapping residual coordination for controlling assistive devices and recovering motor functions *Neuropsychologia* **79** 364–76
[41] Farshchian A, Gallego J A, Miller L E, Solla S A, Cohen J P and Bengio Y 2019 Adversarial domain adaptation for stable brain-machine interfaces *7th Int. Conf. Learn. Represent.* pp 1–14
[42] Jain S, Farshchiansadegh A, Broad A, Abdollahi F, Mussa-Ivaldi F and Argall B 2015 Assistive robotic manipulation through shared autonomy and a Body-Machine Interface *IEEE Int. Conf. Rehabil. Robot.* **2015** 526–31
[43] Donchin O, Francis J T and Shadmehr R Quantifying generalization from trial-by-trial behavior of adaptive systems that learn with basis functions: theory and experiments in human motor control 2003 *J. Neurosci.* **23** 9032–45
[44] Pierella C, Casadio M, Solla S A and Mussa-Ivaldi F A 2019 The dynamics of motor learning through the formation of internal models *PLoS Comput. Biol.* **15** e1007118
[45] Scholz J P and Schöner G 1999 The uncontrolled manifold concept: identifying control variables for a functional task *Exp. Brain Res.* **126** 289–306
[46] Todorov E and Jordan M I 2002 Optimal feedback control as a theory of motor coordination *Nat. Neurosci.* **5** 1226–35
[47] Bernstein N 1966 *The Co-Ordination and Regulation of Movements* (Oxford: Pergamon Press)
[48] Razavian R S, Ghannadi B and McPhee J 2019 On the relationship between muscle synergies and redundant degrees of freedom in musculoskeletal systems *Front. Comput. Neurosci.* **13** 1–12
[49] Härdle W and Vieu P 1992 Kernel regression smoothing of time series *J. Time Ser. Anal.* **13** 209–32
[50] Lipton Z C, Berkowitz J and Elkan C 2015 A critical review of recurrent neural networks for sequence learning (arXiv: 1506:00019)
[51] Segil J and Weir R 2015 Novel postural control algorithm for control of multifunctional myoelectric prosthetic hands *J. Rehabil. Res. Dev.* **52** 449
[52] Tenenbaum J B, De Silva V and Langford J C A global geometric framework for nonlinear dimensionality reduction 2000 *Science* **290** 2319–23